To: Dr. Saundra F. DeLauder, Dean of Graduate Studies and Research

The members of the Committee approved the Thesis of _____ Penglong Xu _____

Student's Name

as presented on ___May 22, 2014___.

Date

We recommend that it be accepted in partial fulfillment of the requirements for the degree of

Master of Science with a major in ___Applied Mathematics___.

_____ Department _Math Sci_ Date _5/29/2014_
Advisor

_____ Department _Math_ Date _5/29/2014_
Member

Paul F. Shlson Department _Math Sci_ Date _6/2/14_
Member

_____ Affiliation _Biology_ Date _5/29/14_
Outside Member

APPROVED

_____ Department _Math_ Date _6/3/14_
Program Director

_____ College _Dale, Nat. Science & Tech._ Date _06/03/14_
Dean

_____ Date _6/5/2014_
Dean, School of Graduate Studies and Research

MAMMOGRAM IMAGE REGISTRATION WITH BEST AFFINE TRANSFORMATION

by

PENGLONG XU

A THESIS

Submitted in partial fulfillment of the requirements for the
degree of Master of Science in
the Applied Mathematics Graduate Program
of Delaware State University

DOVER, DELAWARE
August 2014

TITLE

DEDICATION

I would like to thank my loving parents and my wife for all their love and support, and for believing in me. And I would also like to thank all of my friends and colleagues for always being there for me.

ACKNOWLEDGEMENTS

ABSTRACT

A novel breast image registration method is proposed to obtain one composite mammogram from several images with partial breast coverage, for the purpose of accurate breast density estimation. The breast percentage density estimated as a fractional area occupied by fibroglandular tissue has been shown to be correlated with breast cancer risk. Some mammograms, however, do not cover the whole breast area, which makes the interpretation of breast density estimates ambiguous. One solution is to register and merge mammograms, yielding complete breast coverage. Due to elastic properties of breast tissue and differences in breast positioning and deformation during the acquisition of individual mammogram, the use of linear transformations does not seem appropriate for mammogram registration. Non-linear transformations are limited by the changes in the mammographic projections pixel intensity with different positions of the focal spot. We propose a novel method based upon non-linear local affine transformations. Initially, pairs of feature points are manually selected and used to compute the best fit affine transformation in their small neighborhood. Finally, Shepherd interpolation is employed to compute affine transformations for the rest of the image area. The pixel values in the composite image are assigned using bilinear interpolations. Preliminary results with clinical images show a good match of breast boundaries, providing an increased coverage of breast tissue. The proposed transformation can be controlled locally. Moreover, the method is converging to the ground truth deformation if the paired feature points are evenly distributed.

TABLE OF CONTENTS

LIST OF TABLES

LIST OF FIGURES OR ILLUSTRATION

Chapter 1

INTRODUCTION

Breast cancer is the most common type of cancer in women worldwide. About one in eight (12%) women in the US will develop invasive breast cancer during their lifetime. In the year of 2013, there is 232,340 new cases of invasive breast cancer in women and 39,620 deaths from breast cancer (women) in the United States [24]. In England, breast cancer rates have increased by 90% since records began in 1971. In 2009 more than 48,400 women were diagnosed with breast cancer in the UK - around 133 women a day; Around 370 men were diagnosed with breast cancer [23]. In general, all women are at risk for breast cancer. The risk of getting breast cancer increases as you age. Most breast cancers and breast cancer deaths occur in women aged 50 and older. Although rare, younger women can also get breast cancer. Fewer than five percent of breast cancers occur in women under age 40. However, breast cancer is the leading cause of cancer death (death from any type of cancer) among women ages 20 to 59 [24].

Breast cancer is a type of cancer originating from breast tissue, most commonly from the inner lining of milk ducts or the lobules that supply the ducts with milk. There are two kinds of breast cancer, one is known as ductal carcinoma which develops from ducts, the other is known as lobular carcinoma which develops from lobules. The most effective treatment for breast cancer is to detect the cancer at an early stage. The survival rate of a patient depends on the tumor size at the time of detection. If the tumor size is large, then the probability for the presence of metastases in vital organs is large [7]. Early detection of breast tumor is good for effective treatment [12].

There are many different imaging methods for breast cancer detection and biopsy of suspicious lesions. X-ray mammography is the main screening tool used for detection and diagnosis of breast cancer. X-ray mammography uses low-energy X-rays (usually around 30 kVp) to examine the human breast, typically through detection of characteristic masses or microcalcifications. During the procedure, the breast is compressed using a dedicated mammography unit. Parallel-plate compression is to reduce the thickness of tissue that x-rays must penetrate to decrease the amount of scattered radiation (scatter degrades image quality), to reduce the required radiation dose, and to hold the breast still (preventing motion blur) to even out the thickness of breast tissue to increase image quality.

Since 1990, the death rate from breast cancer has decreased by almost 30% and the study in Sweden and the Netherlands shows two-thirds of the decrease in cancer deaths due to mammography screening [13]. Keen indicated that repeated mammography starting at age 50 saves about 1.8 lives over 15 years for every 1,000 women screened [17]. However, mammography still has some risks and limitations such as false positives, false negatives and radiation exposure. The statistics about mammography and women between the ages of 40 and 55 are the most contentious. A 1992 Canadian National Breast Cancer Study showed that mammography (conducted in the 1980s) had no positive effect on mortality for women between the ages of 50 and 60 [16]. There is evidence that clearly shows that there is over-diagnosis of cancer when women are screened. An estimate of this over-diagnosis is 10 breast cancers diagnosed and unnecessarily treated per life saved when 2000 women are screened for 10 years [10]. These cancers would never have affected these women in their lifetimes. Currently, the American Cancer Society, the American College of Radiology, and the

raphy for women beginning at age 40 [14]. The National Cancer Institute encourages mammography every one to two years for women ages 40 to 49 [22]. For this reason, the radiologist will try to avoid mammography by using ultrasound or magnetic resonance imaging (MRI). In order to optimize these systems in clinically relevant tasks, anthropomorphic breast phantoms would be very beneficial for preclinical validation of novel imaging modalities.

According to both preclinical and clinical studies, newly developed imaging modalities are needed for validation and optimization. Preclinical studies usually involve analysis of the images of physical breast phantoms that is simulate appropriate physical properties of breast tissues. Due to their simplified design, such phantoms offer a very limited representation of the complex anatomy of the breast. An alternative breast phantom based upon a realistic simulation of the breast anatomy has been used for preclinical imaging modalities.

The following two examples can illustrate the potential benefit of realistic breast anatomy simulation. First, we have used simulated images of our anthropomorphic software breast phantom for the optimization of a commercial digital breast tomosynthesis (DBT) reconstruction method [2]. Selection of reconstruction parameters to optimize the estimation of breast density was based upon a comparison between the reconstructed phantom slices and the ground truth information of the simulated tissues. In another application, the geometric accuracy of DBT reconstruction was validated in the presence of realistically simulated parenchymal patterns [3]. The clinical realism of our phantom is reflected in the appearance of the parenchymal pattern which makes up the anatomical noise in projection mammography. In mammography, the parenchymal pattern, formed by the overlapping projections of breast anatomical

structures [21], exhibits a power spectrum with $1/f^\beta (\beta \approx 3)$ proportionality to the spatial frequency [5].

Several methods for 2D simulation of parenchymal patterns have been proposed in the form of clustered lumpy background [4, 6] or random fields based upon a $1/f$ process [11]. Due to their 2D approach, these methods can produce images which successfully match some statistical properties of clinical mammograms. However, they cannot simulate the appearance of the same breast when imaged by different modalities, especially 3D imaging modalities. The anthropomorphic breast phantom has limitation is that they mimic the appearance of a unique breast clinical image. Hence they cannot sufficient represent the variety of breast sizes, shapes, compositions, and parenchymal information. It would be very difficult to get patient specific physical phantoms due to the expensive materials and time-consuming production process.

Some mammograms do not cover the entire patients breast, e.g., due to large breast size in comparison to the x-ray imaging detector. This is of particular importance for the estimation of breast density, a biomarker of breast cancer risk. Partial breast visualization limits our ability to calculate breast density. One solution is to register and merge such partial mammograms to yield complete breast coverage. Registration of mammograms is challenging because the mammogram is a 2D projection of non-rigid breast tissues. As a result, the 3D arrangement of the breast tissue is not exactly replicated in partial projections of large breasts. This is further complicated by differences in mammographic compression between images.

Registration techniques can be classified into the following 3 categories.

1. Feature based techniques

Feature based image registration is to find correspondence between image features such as points, lines, and contours. There are essentially four steps to do the image registration:

a. Feature detection

This involves finding salient features in the two images to be registered. An interest point detector is firstly employed to detect characteristic points in the image. These may include corner points and edges etc. Ideally, we want these points to be invariant to geometric and photometric transformations.

b. Feature matching

Once features have been detected in the two images, the next step is to match them or establish correspondence. The common approach to feature matching is to build local descriptors around the feature point and then to match the descriptors. This is an important step because the percentage of correct matches identified here determines how well the transformation can be estimated in the next step. Common matching methods include simple Euclidean distance matching, invariant moments and nearest neighbor based matching.

c. Transform model estimation

Once feature correspondence has been established, the next step is to solve for the parameters of some global transformation. Usually this involves finding the translation, rotation and scale parameters to transform one image to another.

d. Image re-sampling and transformation

The final step of any registration algorithm involves the actual mapping of one image to the other using the transform model estimated in step 3.

2. Intensity based algorithms

Intensity based methods compare intensity patterns in images via correlation metrics and register entire images or sub images. If sub images are registered, centers of the corresponding sub images are treated as corresponding feature points. The first step is to produce a good initial nonrigid registration using a landmark initialization step. After the landmark initialization step, the next step is used to produce a consistent set of forward and reverse transformations. The last step is to use the consistent intensity registration to refine the transformations based on the matching of the intensities of the images.

3. Hybrid methods

Hybrid methods integrate the merits of both feature based and intensity based methods. These methods focus on incorporating user provided or automatically extracted geometric feature constraints into the intensity-based energy functionals to achieve smoother and faster optimization.

For all of these registration techniques, a transformation must be determined so that the points in the warped image can be related to their corresponding points in the reference image. Based on the number of degrees of freedom, the transformation models can use linear transformation (rigid and affine), elastic models or diffeomorphic transformations. Local controls cannot be achieved from the linear transformation model as the global parameters are computed for the entire image. The elastic model offers high order control, but the performance of elastic models is a balance between flexibility and computational complexity. Diffeomorphic transformations, which preserve topology, have resulted in good performance in a number of applications including brain MRI image registration.

The main difficulty of feature-based methods is to extract and match intrinsic feature points from mammograms. as there are no significant landmarks in a mammogram except the nipple. In this paper. a novel feature based approach, non-linear local affine transformation, is proposed to obtain a composite image from several images with partial breast coverage. Feature points are manually selected near a nipple, breast boundary and inside the breast based upon visual similarity in both mammograms. Affine transformations between sets of feature points are then computed. Finally, Shepard interpolation [19] is used to extend affine transformations to the entire breast. The pixel values in the composite image are assigned using the average of different images. Results with clinical images show that the resulting image consists of the non-overlapping parts of the original images and that the texture of the composite part of the overlapping parts has a good agreement with the original images.

Qualitative testing is presented on selected images from the ACRIN DMIST database [18]. This work was tested with anonymized images obtained from IRB ethical review. A clinical image was split into two overlapping partial images; one partial image was transformed (the warped image), while the other one was not modified (the reference image). Those images were treated as a pair of mammograms with different coverage.

Chapter 2

METHODOLOGY

2.1 Extraction of feature points

Our algorithm requires the feature points be extracted prior to registration, and the registration result depends on the reliability and the accuracy of the extracted features. Automatic identification and extraction of feature points are difficult to perform due to the non-linear compression deformation and the lack of significant landmarks in mammograms (Fig. 2.1). Usually, the features can be the center of Return On Investment (ROI), crossing points, end points and middle points. We observe the prominent features (such as ducts and blood vessels) from both images, the crossing points are determined upon visual similarity in both mammograms. Due to compression and different positions, the coordinates of those crossing points may be different in two mammograms, but the orientation of feature and the local curvature of the crossing points are most likely to be preserved. The advantage of our manual extraction is that the correspondence of the two sets of the feature points can be established during the extraction step. We also select other features (end points and middle points) in a small neighborhood around the selected crossing points. Subsequently, the deformation between two set of feature points can be estimated.
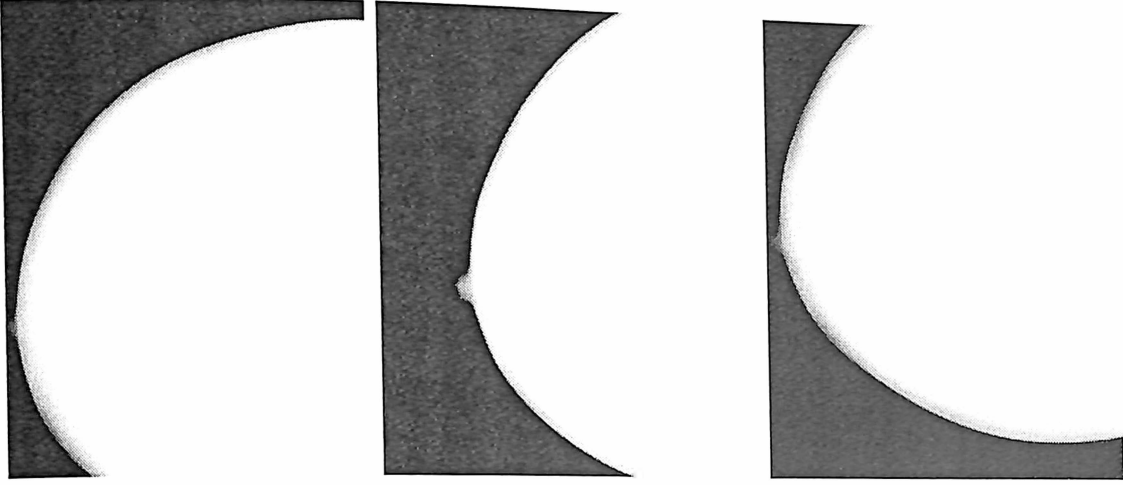
Figure 2.1: Three clinical images of the same patient from ACRIN DMIST database demonstrating partial breast coverage

$XSETS1$	137.37 12.89	138.78 13.74	138.22 12.42	140.57 14.77	139.07 12.33
$YSETS1$	95.13 12.7	96.07 13.93	96.07 12.04	97.29 14.21	96.63 11.76
$ZSETS1$	119.68 49.3	120.81 50.06	120.44 48.55	121.57 50.81	121.19 48.55
$XSETS2$	150.73 2.82	151.86 4.23	149.89 2.26	151.02 4.52	152.43 5.36
$YSETS2$	107.92 3.86	108.49 5.08	106.04 2.35	108.2 5.36	107.92 6.3
$ZSETS2$	134.93 39.52	136.34 42.34	133.51 38.39	135.21 42.06	135.49 42.91

Table 2.1: The pixel values of two sets of feature points which selected form the three clinical images

2.2 Affine transformation

Suppose for some square matrices A, there exists a matrix B such that $AB = BA = I$ where I is the 2×2 identity matrix. If matrix B exists, it is easy to show that it is unique. Such a matrix A is called invertible or nonsingular, and the corresponding matrix B, denoted by A^{-1}, is called the inverse of A. As $AA^{-1} = A^{-1}A = I$, the matrix A^{-1} is also invertible and A is its inverse. Let A be an invertible matrix, let b be a vector, and let $f : R^2 \to R^2$ be defined via $x \mapsto Ax + b$. For any vector y, the following are all equivalent.

$f(x) = y$;

$Ax + b = y$;

$Ax = y - b$;

$A^{-1}(Ax) = A^{-1}(y - b)$;

$(A^{-1}A)x = A^{-1}y - A^{-1}b$;

$Ix = A^{-1}y - A^{-1}b$;

$x = A^{-1}(y - b)$.

We conclude that f^{-1} exists and can be given by $f^{-1}(x) = A^{-1}(x-b)$. Therefore, both f^{-1} and f are bijections on R^2, called transformations of the plane. A transformation f of the plane of the form $f(x) = Ax + b$ where A is an invertible matrix is called an affine transformation of the plane.

Corollary 2.2.1 *A composition of affine transformations is an affine transformation.*

Let $f(x) = Ax + a$ and $g(x) = Bx + b$ be affine transformations. Then $(g \circ f)(x) = g(f(x)) = B(Ax + a) + b = (BA)x + (Ba + b)$. Since A and B are invertible matrices, BA is invertible. This can be seen in several ways.

$$(A^{-1}B^{-1})(BA) = A^{-1}(B^{-1}B)A = A^{-1}(I)A = A^{-1}A = I,$$

and similarly, $(BA)(A^{-1}B^{-1}) = I$. Thus,

$$(BA)^{-1} = A^{-1}B^{-1}.$$

Therefore BA is invertible, and we conclude that $g \circ f$ is an affine transformation.

$\square$

In R^2, an affine transformation is a function which preserves points, straight lines and planes. Also, sets of parallel lines remain parallel after an affine transformation. An affine transformation does not necessarily preserve angles between lines or distances between points, though it does preserve ratios of distances between points lying on a straight line. In general, an affine transformation is a composition of rotations, translations, dilations, and shears.

Affine transformation is mostly used in image processing. Under certain assumptions, an affine transformation can be used to align two images and approximate the effects of perspective projection. The main application of affine transformation is used in automatic image registration which is to perform the image registration task without the guidance and intervention of users [8]. The need of automatic image registration comes from widespread applications. For example, one has to use efficiently automatic image registration method to glue together the tremendous amount of satellite images from the Earth Observing System (EOS) program. The following theorem [9] provides the properties of affine transformations.

Theorem 2.2.1 *Let $f(x) = Ax + b$ be an affine transformation. Then f*

(1) maps a line to a line,

(2) maps a line segment to a line segment,

(3) preserves the property of parallelism among lines and line segments,

(4) maps an n-gon to an n-gon,

(5) maps a parallelogram to a parallelogram,

(6) preserves the ratio of lengths of two parallel segments,

(7) preserves the ratio of areas of two figures.

2.3   Best affine transformation

Due to the fact that two pictures can not exactly match each other, we can improve the affine transformation to the best affine transformation. We attempt to make the error between the two pictures be as small as possible. Given two sets of feature points in two images that need to be registered, we assume the deformation between them can be approximated by affine transformation, which can be considered as a first-order approximation of the true transformation resulting from breast projection. For a real-valued function f with domain S, $argmin_{x \in S} f(x)$ is the set of elements in domain S that achieve the global minimum in S:

$$argmin_{x \in S} f(x) = \{x \in S : f(x) = min_{y \in S} f(y)\} \tag{2.1}$$

Denote the two images obtained from different angle and different compression by I_1 and I_2, and assume $S_1 = \{X_1, X_2, \cdots, X_n\}$ be a set of feature points in I_1 (reference image), and $T_1 = \{Y_1, Y_2, \cdots, Y_n\}$ be the corresponding set in I_2 (warped image). Particularly, X_1 and Y_1 are the crossing points in each set, called the centers of S_1 and T_1. The crossing points X_1 and Y_1 are used to calculate matrix A and vector b. Then A and b are used to obtain the affine transformation on the two sets S_1 and T_1. The affine transformation $\varphi : \varphi(x) = Ax + b$ mapping S_1 into T_1 can be obtained by solving the optimization problem:

$$argmin_{A \in R^2 \times R^2, b \in R^2} \sum_{j=1}^{n} \| AX_j + b - Y_j \|^2, \qquad (2.2)$$

where A is a 2×2 matrix including scaling and rotation, $b \in R^2$ is a translation vector. For non-invertible matrix, please see the following theorem [9].

Theorem 2.3.1 *Let A be a real 2×2 matrix. Then the following statements are equivalent:*

(1) $detA = 0$

(2) The row vectors of A are collinear.

(3) The column vectors of A are collinear.

The solution of the above optimization problem (2.2) can be expressed [20] as:

$$[A, b] = ([Y]_{2 \times n}[X, 1]_{n \times 3})_{2 \times 3}([X, 1]_{3 \times n}^{T}[X, 1]_{n \times 3})_{3 \times 3}^{-1}, \qquad (2.3)$$

where $X = [X_1, X_2, \cdots, X_n]$ and $Y = [Y_1, Y_2, \cdots, Y_n]$.

Proof: Set $M = [X, 1]_{2 \times 3}$ and $u = [A, b]^T$, then

$$argmin_{A \in R^2 \times R^2, b \in R^2} \sum_{j=1}^{n} \| AX_j + b - Y_j \|^2 = argmin_u \| Mu - Y \|^2 . \qquad (2.4)$$

Write $M = QR$, where Q is an 2×3 matrix with orthogonal rows, and R is an 3×3 upper triangular invertible matrix.

First note that we can write $Y = y_1 + y_2$, where $y_1 = QQ^TY$, and $y_2 = Y - QQ^TY$. Since $Q^TQ = I$,

$$Q^T y_1 = Q^T QQ^T Y = Q^T Y. \qquad (2.5)$$

But on the other hand

$$Q^T y_2 = Q^T (Y - QQ^TY) = Q^T Y - Q^T QQ^T Y = Q^T Y - Q^T Y = 0. \qquad (2.6)$$

Thus

$$< Mu, y_2 >= u^T M^T y_2 = u^T R^T Q^T y_2 = 0. \qquad (2.7)$$

and

$$< y_1, y_2 >= Y^T QQ^T y_2 = 0. \qquad (2.8)$$

So

$$\begin{aligned}
argmin_u &\| Mu - Y \|^2 \\
&= argmin_u \| (Mu - y_1) \|^2 + \| y_2 \|^2 - 2 < Mu - y_1, y_2 > \\
&= argmin_u \| (Mu - y_1) \|^2 + \| y_2 \|^2 \\
&= argmin_u \| (Mu - y_1) \|^2,
\end{aligned} \qquad (2.9)$$

because $\| y_2 \|^2$ is independent of u; that is, adding $\| y_2 \|^2$ changes the objective value at the minimum, but does not change the *argmin*. Now make the substitution $a = Ru$:

$$argmin_u \| Mu - Y \|^2 = argmin_a \| Qa - y_1 \|^2 . \tag{2.10}$$

Since $y_1 = Q(Q^T Y)$, $argmin_a \| Qa - y_1 \|^2$ has solution given by $a = Q^T Y$ (with objective value $\| Qa - y_1 \|^2 = 0$), and so $argmin_u \| Mu - y_1 \|^2 = R^{-1} Q^T y_1$. Recall $Q^T y_1 = Q^T Y$, so

$$argmin_u \| Mu - Y \|^2 = R^{-1} Q^T Y. \tag{2.11}$$

So $u = R^{-1} Q^T Y$.

Therefore we have the solution

$$[A, b] = ([Y]_{2 \times n} [X, 1]_{n \times 3})_{2 \times 3} ([X, 1]_{3 \times n}^T [X, 1]_{n \times 3})_{3 \times 3}^{-1}. \tag{2.12}$$

$\square$

Similarly, for each corresponding pairs of feature sets $(S_1, T_1), (S_2, T_2), \cdots, (S_k, T_k)$, we can also obtain the best affine transformations $\varphi_1, \varphi_2, \cdots, \varphi_k$ that minimize the least square error. Note that if we consider $\{\varphi_i\}$ as a basis, then for an arbitrary point in I_1, we can find its affine transformation by combining the basis with different non-linear weights. (see equation (2.14) below).

2.4 Non-linear Local Affine Transformation

The Shepard interpolation [19], which is a simple case of inverse distance weighting to assign value to unknown points based on given points, is employed to compute the local affine transformation φ for each non-feature point in the image. Shepard's

Algorithm 1: $[A, b] = bestAffineTrans(XSETS1, YSETS1, t))$

Input: $XSETS1, YSETS1, t$

/* t is the weight of first pair of the two sets X and Y ; */

Output: $A and b is the best affine transfomation between X and Y$

- Set m and n as the size of X

- Compute the weight for other pair as $s = (1 - t)/(n - 1)$

- Compute the minimize the least square error.

- Return $[A, b] = ([Y]_{2 \times n}[X, 1]_{n \times 3})_{2 \times 3}([X, 1]_{3 \times n}^T[X, 1]_{n \times 3})_{3 \times 3}^{-1}$.

Interpolation Scheme: Let $F(P)$ be a function of the point $P = (x, y)$ defined for all P in the real plane R^2, and let $(P_i)_{i=1}^N$ be any finite collection of distinct points in R^2. Denote the value of F at P_i by F_i, and let $r_i = |P - P_i|$ be the distance between P_i and the generic point P in R^2:

$$r_i = [(x - x_i)^2 + (y - y_i)^2]^{1/2}. \tag{2.13}$$

Assume X_i and Y_i are the centers of S_i and T_i, i.e., the affine transformation of X_i is φ_i, obtained from equation (2.3). For any other point Z in I_1, its corresponding local non-linear affine transformation φ is defined as

$$\varphi(Z) = \begin{cases} \frac{\sum_{i=1}^k d_i^{-\alpha} \varphi_i}{\sum_{i=1}^k d_i^{-\alpha}}, & if (\forall i) Z \neq X_i, \\ \varphi_i, & if (\exists i) Z = X_i, \end{cases} \tag{2.14}$$

where $d_i = |X_i - Z|$ is the Euclidean distance between X_i and Z. Note that non-linear deformation mapping φ is continuous since $\lim_{Z \to X_i} \varphi(Z) = \varphi_i$. Moreover, the partial derivatives with respect to two coordinates of φ exist at all the points if $\alpha > 1$. We choose the default value of α as 2 for convenience of computation. The function $\varphi(Z)$

can be considered as the first order approximation of the ground truth deformation in a small neighbor of Z. It converges to the ground truth deformation when the number of neighbors k is large enough and the feature points are evenly distributed. Note also that φ can be expressed locally as a linear combination of affine transformations. Moreover, local controls can be achieved if we add or delete feature sets in the region of interest.

The purpose of our image registration is to map both I_1 and I_2 into one region to get composite image, say I_c. I_1 can be mapped to I_c by a translation transformation. The non linear local affine transformation φ is used to estimate the mapping between I_2 and I_c, which will change the shape of image I_c.

In order to initialize the size of I_c, we have to determine the maximum and minimum value of I_2 under the local affine transformation $\varphi(x)$, where x can be represented by linear combination of four corner points c_j of I_2,

$$x = \sum_{j=1}^{4} w_j c_j, \qquad \varphi(x) = \varphi(\sum_{j=1}^{4} w_j c_j) = \sum_{j=1}^{4} w_j \varphi(c_j). \qquad (2.15)$$

According to equation (2.14), we know that $\varphi(x)$, the local affine transformation at point x, is the linear average of φ_i with weight 1. Therefore,

$$max_x\varphi(x) = max_i(max_j\varphi_i(c_j)), \qquad min_x\varphi(x) = min_i(min_j\varphi_i(c_j)). \qquad (2.16)$$

Now we can classify I_c into four different regions R_1: the points x that have only inverse image y in I_1; R_2: the points x with inverse image z only from I_2; R_3: the points x that have inverse images y both in I_1 and in I_2; R4: the points that do not have any inverse image. The following strategy is used to assign gray values to the points in I_c,

$$I_c(x) = \begin{cases} I_1(y), & x \in R_1, \\ I_2(z), & x \in R_2, \\ \frac{I_1(y)+I_2(z)}{2}, & x \in R_3, \\ 0, & x \in R_4. \end{cases} \tag{2.17}$$

Algorithm 2: $Image = whole\_breast\_generation(A, b, imageI1, imageI2)$

Input: A, b, $imageI1$, $imageI2$

    /* $imageI1$ will have non-linear local affine transformation and $imageI2$ will have only shift ; */

Output: Image is combined $imageI1$ and $imageI2$

Determine the size of new image and Initialization of boundary of new image

Set $size1$ and $size2$ are the size of the new image

Set $shift1$ and $shift2$ are the size shift from $imageI2$ to the new image

for *each $i = 1$ to $size1$* **do**
    for *each $j = 1$ to $size2$* **do**
        y is a 1 by 2 vector, which is any point in the image;
        x is the corresponding point of y in another image after local Affine Transformation
        (Shepard interpolation for affine transformation at crossing points);
        x0 is the round of x;
        if $x0(1) >= 1$ && $x0(1) <= nrow$ && $x0(2) >= 1$ && $x0(2) <= ncol$
        then
            Image(i,j)=image(x0(1),x0(2));
        end
    end
end

for *each $i = 1 + shift1$ to $nrow + shift1$* **do**
    for *each $j = 1 + shift2$ to $ncol + shift2$* **do**
        if $Image(i, j) == 0$ **then**
            $Image(i, j) = image(i - shift1, j - shift2)$
            else if $image(i - shift1, j - shift2) > 2000$ **then**
                $Image(i, j) = (Image(i, j) + image4(i - shift1, j - shift2))/2$
        end
    end
end

return $Image(i, j)$

The simplest validation is obtained from examination of the pixel-wise brightness difference between the reference image and the transformed warped image. However, such technique does not provide good performance for mammogram registration due to the 3D various projections of the breast tissues. Even if the positions of the image features are matched in the warped image and the reference image, the pixel brightness of same features will be different since the path of X-ray is different. As an initial validation, individual clinical images were transformed to mimic partial coverage as illustrated in (Fig. 2.2). A clinical image is split into two overlapping partial images. One partial image was transformed by non-linear compression deformation (the warped image) and another was not modified (the reference image). According to the pixel values of the each points of the partial image, we then changed the gray values of each points to get the warped image. The warped image and the reference image were treated as a pair of mammograms with different coverage. The registration error can be computed as the difference between the original image and the composite image after the registration.
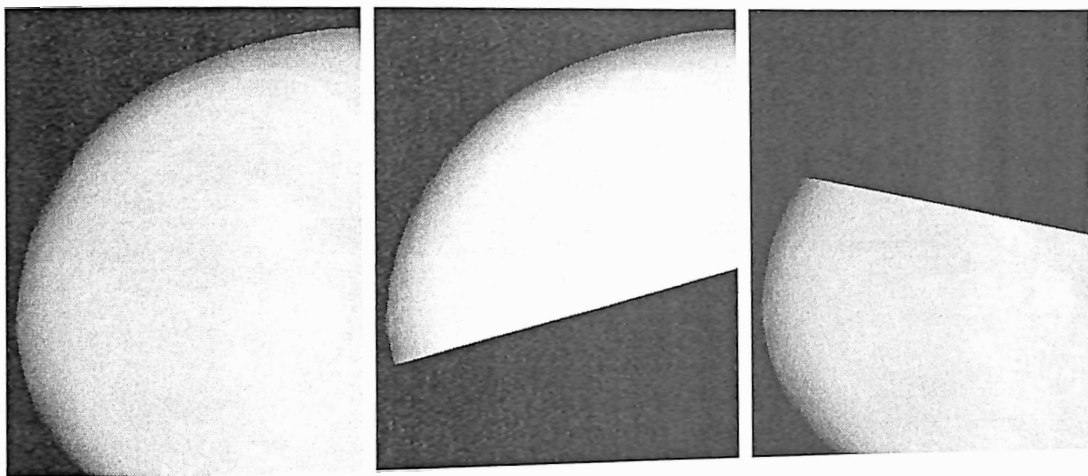
Figure 2.2: Original image and partial images (1 and 2) for validation

Chapter 3

RESULTS AND DISCUSSION

In this section we present preliminary results using the proposed approach applied to clinic mammograms taken from the ACRIN DMIST database of mammograms. This work is part of a larger study of health disparities in breast cancer risk. In that project, breast percent density and parenchymal texture of minority women and age matched Caucasian controls from the ACRIN DMIST database [18] are being compared.

Fig. 3.1(a) and Fig. 3.1(b) illustrate the registration of two images from a large breast using the proposed non-linear local affine transformation with 9 pairs of feature sets. The effect of the choice of reference image is shown. Fig. 3.1(c) shows the composition of 3 partial views that covers the whole breast.

Fig. 3.2 illustrates the qualitative comparison of the proposed method with the result of Advanced Normalization Tools (ANTs) [1]. ANTs that computes the unsupervised optimal diffeomorphic transformation by minimizing the similarity measure between the warped image and the reference image. The registered image of the warped image (Fig. 3.2(a)) and the reference image (Fig. 3.2(a)) is shown in Fig. 3.2(c). Fig. 3.2(c) illustrates the result of ANTs.

Fig. 3.3 illustrates the comparison of the original and the registered images. The reference image (Fig. 3.3(a)) and the warped image (Fig. 3.3(b)) are obtained from Fig. 2.2(c). Fig. 3.3(c) is the original image from Fig. 2.2(a). Fig. 3.3(d) illustrates the registered image using the proposed method, and Fig. 3.3(e) shows the difference between the composite and the original images.
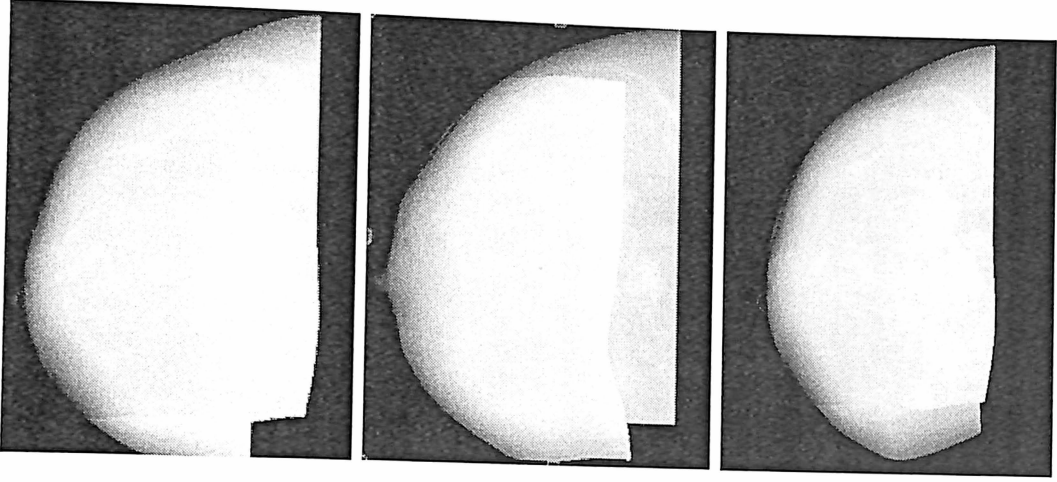
Figure 3.1: a,b: Two partial images combined following registration, showing the effect of the choice of reference image. c: The same breast showing the composition of three images in figure 1 after logarithm of gray scale values.

To date, we have been able to achieve anecdotal results that support continued development and testing of this new method. Fig. 3.1(a) and Fig. 3.1(b) suggests that the proposed method is robust, since the results of registration are similar regardless of the choice of the reference image (comparing Figs. 3.1(a) and 3.1(b)). Fig. 3.1 indicates that the observable features, especially the nipple and the boundary of skin, have good agreement. Fig. 3.2 suggests that the results of the proposed method are comparable to the results of the diffeomorphic transform implemented using ANTs(an open source software package). Particularly, the textures of the warped image are preserved in the registered images, and the shapes of the registered images are similar as the reference image. The proposed method has difficulties in registering some regions of the image (corresponding to region R_4, see equation (2.6)). Fig. 3.3 suggests that the features in the composite image show good agreement. The registration error is small in the region of overlap (the upper part of the registered image), since we can extract the corresponding feature points only from this region.
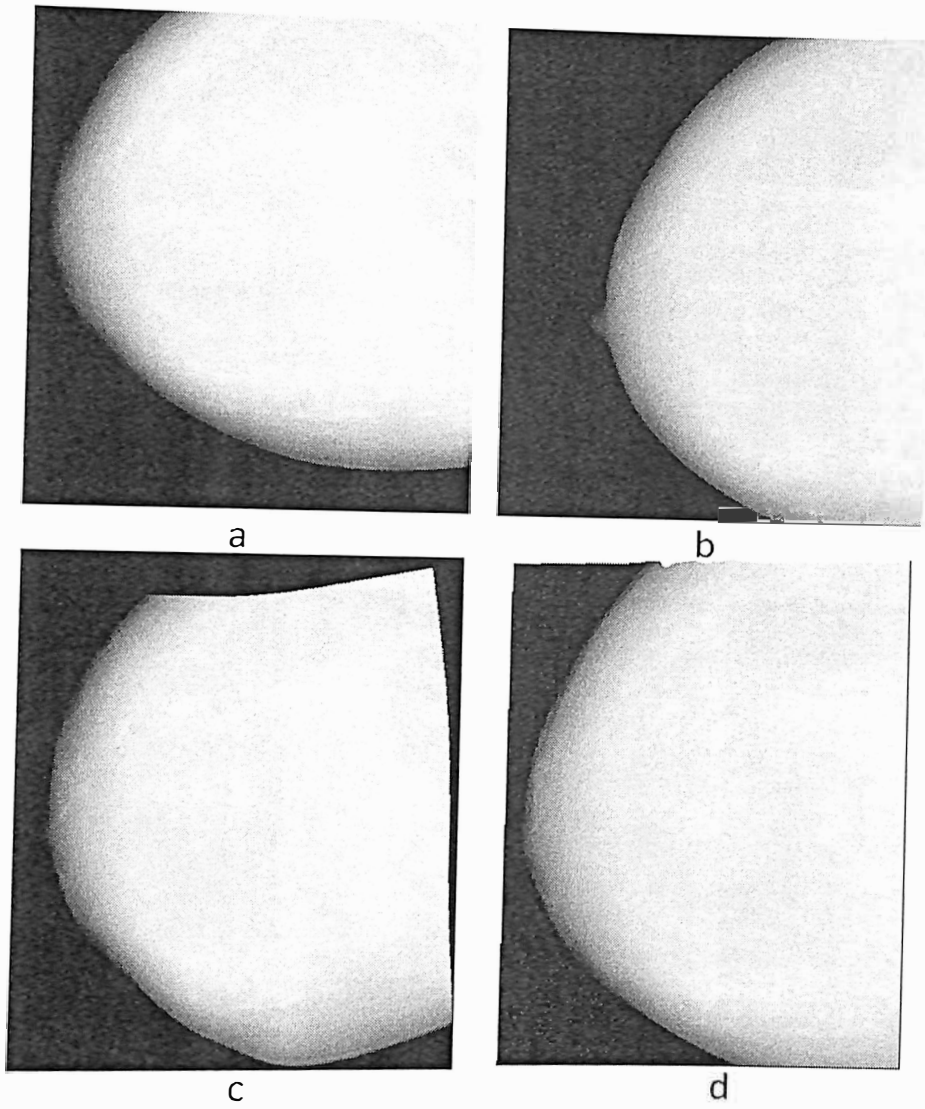
Figure 3.2: Warped image (a), reference image (b) and the result using the proposed method (c) and Advanced Normalization Tools (ANTs) (d).

Reference

Warped
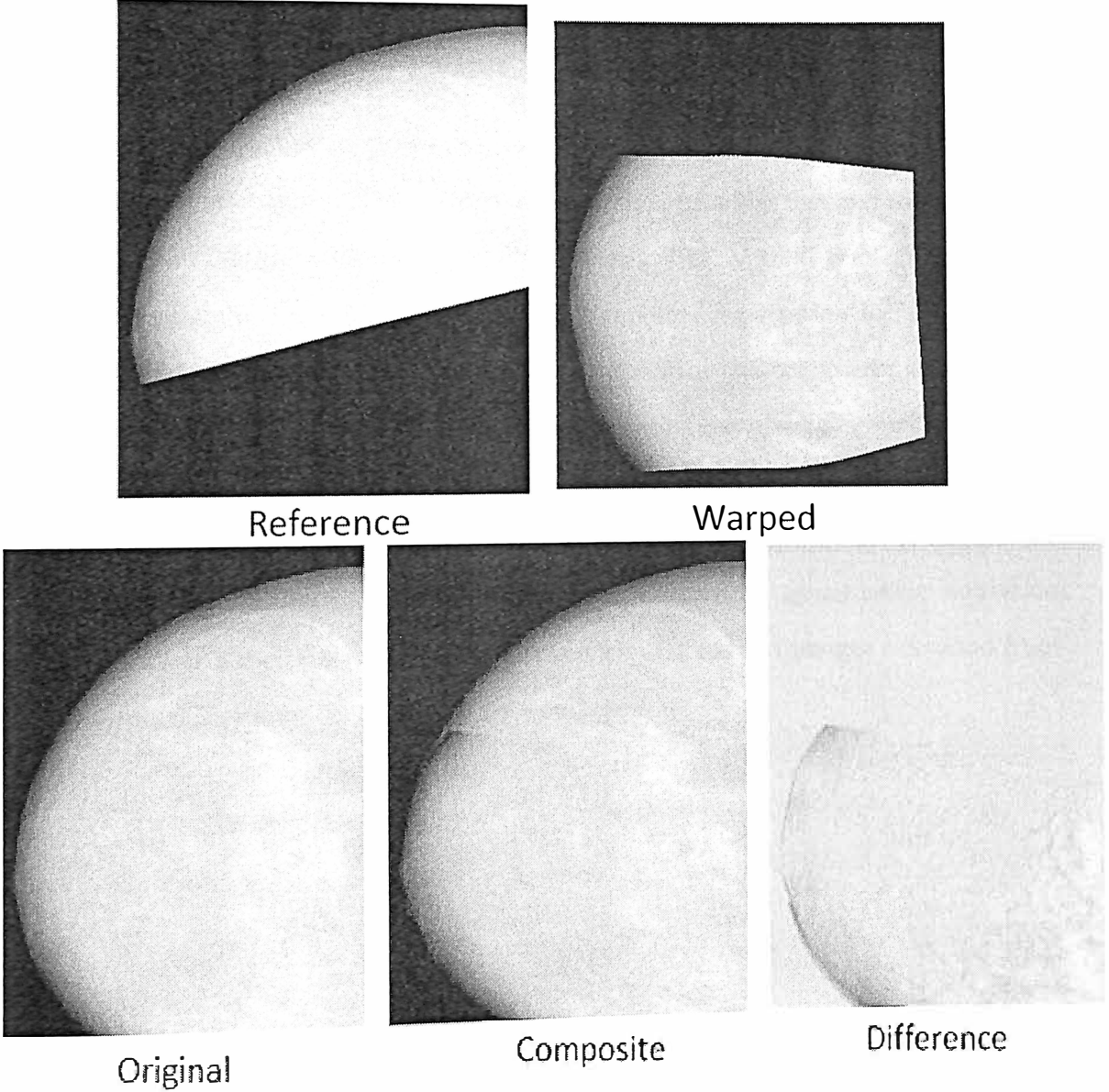
Original

Composite

Difference

Figure 3.3: Example validation.

Chapter 4

CONCLUSION

A novel registration task is proposed, and two methods are compared in this task. This study indicates that our newly proposed method provides fast and comparatively accurate registration of overlapping breast images. The method is effective whether used stand alone or for initialization of other modern registration techniques (e.g., diffeomorphic transformation). The major drawback of the proposed method is the need for manual extraction of feature points. In our future work, we will apply the technique to more images in the DMIST database and develop statistical measures of the registration accuracy which is needed for automatic feature selection (e.g., SIFT algorithm [15]). Finally, we plan to perform more extensive quantitative validation of the proposed algorithm on a series of reference and warped images extracted from all the applicable images in the ACRIN database.

REFERENCE LIST

[1] Avants BB, Tustison, N.J., Song, G., Gee, J.C. ANTS: Advanced Open-Source Normalization Tools for Neuroanatomy. *Penn Image Computing and Science Laboratory*

[2] Bakic, P. R., S. Ng, P. Ringer, A.-K. Carton, E. F. Conant, and A. D. A. Maidment, Validation and Optimization of Digital Breast Tomosynthesis Reconstruction using an Anthropomorphic Software Breast Phantom, *SPIE Medical Imaging: Physics of Medical Imaging*, edited by E. Samei and N. Pelc, Vol. 7622 San Diego, CA, 2010.

[3] Bakic, P. R., P. Ringer, J. Kuo, S. Ng., and A. D. A. Maidment, Analysis of Geometric Accuracy in Digital Breast Tomosynthesis Reconstruction, *IWDM*, 6136, 62-69, Springer, Girona, Spain, 2010.

[4] Bochud, F., Abbey, CK, Eckstein, MP. Statistical texture synthesis of mammographic images with clustered lumpy backgrounds *Opticals Express*, 4(1), 1999.

[5] Burgess, A. E. Mammographic structure: Data preparation and spatial statistics analysis, *SPIE Medical Imaging: Image Processing*, edited by K. M. Hanson, San Diego, CA, 1999.

[6] Castella, C. et al., Mammographic texture synthesis: Second-generation clustered lumpy backgrounds using a genetic algorithm *Opticals Express*, 16(11), 7595C7607, 2008.

[7] Duncan W, Kerr CR The curability of breast cancer *Br Med J*, 2(6039):781C783, 1976.

[8] Fengshan Liu, Xiquan Shi, Zhongyan Lin, and Andrew Thompson Affine Transformation Method In Automatic Image Registration, *NOVA.* pp. 141-152, 2006.

[9] George Bebis, Michael Georgiopoulos, Niels da Vitoria Lobo, and Mubarak Shah, Learning Affine Transformations, pp. 3576-3581, 1999.

[10] Gotzsche PC, Nielsen M Screening for breast cancer with mammography *Cochrane Database Syst Rev*, (1): CD001877, 2011.

[11] Heine, J., Deans, SR, Veithuizen, RP, Clarke, LP., On the statistical nature of mammograms, *Medical Physics*, 26(11). 2254-2265, 1999.

[12] Kaiser WA, Fischer H, Vagner J, Selig M Robotic system for biopsy and therapy of breast lesions in a high-field whole-body magnet resonance tomography unit. *Invest Radiol*, 35(8):513C519, 2000.

[13] Kopans DB Why the critics of screening mammography are wrong *Diagnostic Imaging*, (12): 18C24, 2009.

[14] Lee, C.H. et al. Breast cancer screening with imaging: Recommendations from the Society of Breast Imaging and the ACR on the use of mammography, breast MRI, breast ultrasound, and other technologies for the detection of clinically occult breast cancer *J. Am. Coll. Radiol.*, 7(1), 18-27. 2010.

[15] Lowe DG. Object recognition from local scale-invariant features. *Proceedings of the International Conference on Computer Vision*. 2. pp. 1150C1157, 1999.

[16] Miller AB, Baines CJ, To T, Wall C Canadian National Breast Screening Study *CMAJ 147*, (10): 1477C8, 1992.

[17] Nick Mulcahy Screening Mammography Benefits and Harms in Spotlight Again *Medscape*, 2009.

[18] Pisano E.D., Gatsonis C, Hendrick E, et al. Diagnostic Performance of Digital versus Film Mammography for Breast-Cancer Screening, *NEJM*, 353:1773-1783, 2005.

[19] Shepard, D. A two-dimensional interpolation function for irregularly-spaced data, *Proc. 23rd National Conference ACM*, 517-524, 1968.

[20] Steven J. Miller The Method of Least Squares, *Mathematics Department Brown University*, 2006.

[21] Wolfe, J. N. Risk for breast cancer development determined by mammographic parenchymal pattern, Cancer 37(5), 2486C2492, 1976.

[22] Screening Mammograms: Questions and Answers National Cancer Institute. Released May 2006; accessed April 9, 2007.

[23] Breast Cancer UK patients diagnosed in 2009.

[24] American Cancer Society (2013) Statistics for 2013.

CURRICULUM VITAE

EDUCATION

Master of Science, Applied Mathematics, Expected: May 2013
Thesis Topic: Mammogram Image Registration with Best Affine Transformation
Advisor: Dr. Fengshan Liu
Delaware State University, Dover, DE

Bachelor of Science, Computer science and technology, July 2011
Changchun University of Technology, Changchun, Jilin, P.R. China

ACADEMIC EXPERIENCE

Graduate Student	Delaware State University Dover, DE, USA	Sep 2011-Present
Research Assistant	Delaware State University Dover, DE, USA	Sep 2011-Present
Tutor	Delaware State University Dover, DE, USA	Sep 2012-Present

Duties including helping students in math lab, tutoring students homework, quizzes and tests.

Teaching Assistant	Delaware State University Dover, DE, USA	Sep 2013-Present

Duties including attending class with students, teaching students homework, quizzes and tests.

RESEARCH INTERESTS

Image registration; Image processing, Breast phantom simulation and Computational geometry.

RELEVANT COURSE WORK

- Real Analysis

- Complex Analysis

- Functional Analysis

- Inverse Problems

- Integral Equations

- Scientific Computation I & II

HONORS AND AWARDS

Delaware State University:

Research Assistantship	Sep 2011-Present
Teaching Assistantship	Sep 2012-2013

Changchun University of Technology:

3rd Prize Fellowship	Aug 2008-Jul 2009
2nd Prize Fellowship	Aug 2009-Jul 2010

EXTRA CURRICULAR ROLE AND SOCIAL ACTIVITIES

Treasurer, DSU Chinese Students and Scholars Association 2012- Present

COMPUTER SKILLS

I am proficient in C and C++ programming languages. I am also highly competent in LaTeX, MATLAB, and a variety of other mathematical software packages.